Supporting Information for

How does the solvent composition influence the transport properties of electrolyte solutions?—$LiPF_6$ and LiFSA in EC and DMC binary solvent

Satoshi Uchida and Tetsu Kiyobayashi

S 1 Numerical data

Table S I: Density, ρ, of the solvent without solute and of the 1.0 mol kg^{-1} $LiPF_6$ and the LiFSA solution at $T/K = 298$

Solvent		$LiPF_6$		LiFSA	
x_{EC}	ρ/g cm^{-3}	x_{EC}	ρ/g cm^{-3}	x_{EC}	ρ/g cm^{-3}
0	1.07	0	1.18	0	1.18
0.123	1.11	0.129	1.21	0.128	1.21
0.239	1.13	0.248	1.24	0.251	1.24
0.356	1.16	0.355	1.27	0.361	1.26
0.458	1.19	0.476	1.29	0.464	1.29
0.564	1.22	0.569	1.32	0.562	1.31
0.663	1.24	0.672	1.34	0.663	1.34

Table S II: Viscosity, η/mPa s, of the solvent without solute and of the 1.0 mol kg^{-1} $LiPF_6$ and the LiFSA solution

Solvent		
x_{EC}	T/K	
	288	298
0	0.83	0.57
0.122	1.00	0.75
0.238	1.12	0.82
0.352	1.28	1.01
0.460	1.47	1.16
0.551	1.74	1.36
0.656	1.88	1.52

Viscosity at T/K > 298 is so low and out-of-range of the equipment that we were not able to measure.

$LiPF_6$						LiFSA					
x_{EC}	T/K					x_{EC}	T/K				
	288	298	308	318	328		288	298	308	318	328
0	2.03	1.60	1.26	0.67	0.54	0	2.01	1.55	1.24	0.68	0.58
0.129	2.59	2.03	1.65	1.15	0.82	0.128	2.44	1.96	1.62	1.19	0.91
0.248	3.40	2.68	2.20	1.72	1.50	0.251	2.98	2.34	1.99	1.55	1.36
0.355	4.06	3.26	2.65	2.07	1.77	0.361	3.81	3.08	2.59	2.07	1.76
0.476	5.21	4.19	3.35	2.64	2.39	0.464	4.25	3.44	2.81	2.23	1.94
0.569	6.23	4.98	4.02	3.15	2.72	0.562	4.97	4.08	3.29	2.67	2.20
0.672	7.14	5.69	4.49	3.60	2.93	0.663	5.88	4.73	3.79	3.01	2.43

Table S III: Specific conductivity, σ/mS cm^{-1} of the 1.0 mol kg^{-1} $LiPF_6$ and LiFSA solution

$LiPF_6$						LiFSA					
x_{EC}	T/K					x_{EC}	T/K				
	288	298	308	318	328		288	298	308	318	328
0	6.4	7.2	8.0	8.7	9.5	0	7.3	8.1	9.1	10.0	10.9
0.129	8.8	10.2	11.6	13.1	14.5	0.128	9.6	11.1	12.5	14.1	15.6
0.248	10.0	11.7	13.5	15.4	17.3	0.251	10.7	12.5	14.4	16.2	18.1
0.355	10.1	12.1	14.2	16.4	18.6	0.361	10.9	12.8	14.9	17.0	19.1
0.476	9.9	11.8	14.2	16.4	18.9	0.464	10.6	12.6	14.8	17.1	19.4
0.569	9.1	11.2	13.6	16.2	18.7	0.562	10.0	12.1	14.3	16.7	19.1
0.672	8.3	10.5	12.9	15.4	18.1	0.663	9.3	11.5	13.7	16.1	18.6

Table S IV: Diffusion coefficient, $D/10^{-10}$ m^2 s^{-1} of Li^+, $PF_6{}^-$, FSA^-, EC and DMC at $T/K = 298$ measured by PGSE-NMR

	Solvent	
x_{EC}	EC	DMC
0		24.8
0.123	18.6	20.6
0.239	16.1	17.8
0.356	13.8	15.4
0.458	12.0	13.5
0.564	10.2	11.4
0.663	9.04	10.1

	LiPF$_6$					LiFSA				
x_{EC}	Li^+	$PF_6{}^-$	EC	DMC	x_{EC}	Li^+	FSA^-	EC	DMC
0	3.76	4.43		9.42	0	3.82	4.30		9.51
0.129	3.10	3.96	5.86	7.66	0.128	3.24	3.99	5.98	7.91
0.248	2.58	3.49	5.00	6.56	0.251	2.79	3.65	5.30	6.81
0.355	2.25	3.17	4.22	5.74	0.361	2.40	3.34	4.55	5.74
0.476	1.85	2.76	3.83	4.64	0.464	2.22	3.21	4.44	5.33
0.569	1.72	2.64	3.53	4.37	0.562	1.94	2.92	3.81	4.53
0.672	1.41	2.29	2.97	3.44	0.663	1.67	2.58	3.38	3.89

Table S V: Fraction in the DMC of the *cis-trans* conformer of DMC, $N_{DMCct}/(N_{DMCct} + N_{DMCcc})$, in the solvent without solute

x_{EC}	$N_{DMCct}/(N_{DMCct} + N_{DMCcc})$
0	0.034
0.124	0.042
0.236	0.048
0.351	0.052
0.464	0.055
0.559	0.057
0.659	0.058

Table S VI: Fraction in the DMC of the *cis-trans* conformer bound to Li^+ (ct-Li), free *cis-trans* conformer (ct-0) and *cis-cis* conformer bound to Li^+ (cc-Li). The free *cis-cis* conformer accounts for the balance.

$LiPF_6$				LiFSA			
x_{EC}	ct-Li	ct-0	cc-Li	x_{EC}	ct-Li	ct-0	cc-Li
0	0.068	0.036	0.191	0	0.066	0.037	0.173
0.129	0.073	0.033	0.193	0.128	0.070	0.033	0.180
0.248	0.066	0.033	0.194	0.251	0.056	0.033	0.177
0.355	0.048	0.039	0.198	0.361	0.033	0.036	0.186
0.476	0.041	0.040	0.194	0.464	0.03	0.037	0.175
0.569	0.036	0.039	0.192	0.562	0.027	0.037	0.184
0.672	0.03	0.039	0.186	0.663	0.027	0.037	0.185

Table S VII: Average solvation number, n_s, of Li^+

$LiPF_6$				LiFSA			
x_{EC}	DMCct	DMCcc	EC	x_{EC}	DMCct	DMCcc	EC
0	0.76	2.12	0	0	0.73	1.92	0
0.129	0.71	1.89	0.82	0.128	0.68	1.75	0.82
0.248	0.56	1.64	1.43	0.251	0.47	1.48	1.36
0.355	0.35	1.43	1.73	0.361	0.23	1.32	1.69
0.476	0.24	1.14	2.10	0.464	0.18	1.04	2.00
0.569	0.18	0.93	2.34	0.562	0.13	0.89	2.27
0.672	0.11	0.69	2.61	0.663	0.10	0.70	2.50

S 2 Raman spectroscopy

Fig. S 1(a) plots the fraction of the *cis-trans* (ct) conformer of DMC, $N_{\mathrm{ct}}/(N_{\mathrm{ct}} + N_{\mathrm{cc}})$, in the solvent without solute determined by the Raman signal intensity and its energy difference from the *cis-cis* (cc) conformer, $E_{\mathrm{ct}} - E_{\mathrm{cc}}$. If we assume thermal equilibrium between the two conformers, the probability of DMC being in conformer, A (= cc or ct), is proportional to the Boltzmann factor $\exp(-E_{\mathrm{A}}/RT)$, where E_{A} is the energy of conformer, A. The fraction of the ct-conformer is hence given by

$$\frac{N_{\mathrm{ct}}}{N_{\mathrm{cc}} + N_{\mathrm{ct}}} = \frac{\exp\left(-\dfrac{E_{\mathrm{ct}}}{RT}\right)}{\exp\left(-\dfrac{E_{\mathrm{cc}}}{RT}\right) + \exp\left(-\dfrac{E_{\mathrm{ct}}}{RT}\right)} \tag{S1}$$

or by solving for $E_{\mathrm{ct}} - E_{\mathrm{cc}}$,

$$E_{\mathrm{ct}} - E_{\mathrm{cc}} = RT \ln\left(\frac{N_{\mathrm{cc}}}{N_{\mathrm{ct}}}\right). \tag{S2}$$

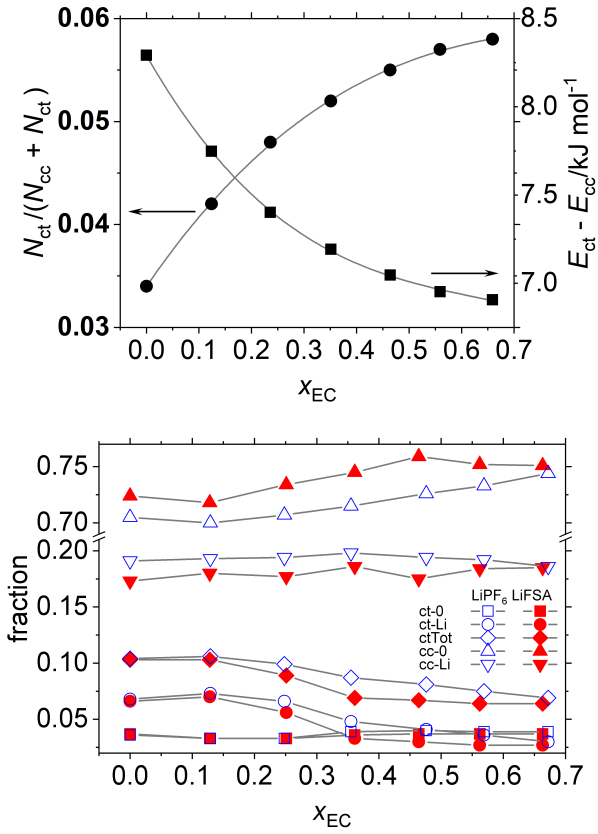

Figure S 1: (a) Fraction of ct-conformer of DMC, $N_{ct}/(N_{cc}+N_{ct})$, in the solvent without solute determined by the Raman signal intensity and the energy difference between two conformers, $E_{ct} - E_{cc}$, calculated based on Eq. (S2). (b) Fraction of each conformer in the 1.0 mol kg^{-1} $LiPF_6$ and LiFSA solution. ct-0: free ct-conformer, ct-Li: ct-conformer bound to Li^+, ctTot: ct-0 + ct-Li, cc-0: free cc-conformer and cc-Li: cc-conformer bound to Li^+.

Fig. S 2 plots the number of solvent molecules (EC and DMC) in the Li^+-solvation shell in which one anion molecule (FSA^- or PF_6^-) is involved, under the assumption that free Li^+ dissociated from the anion is solvated by exactly four solvent molecules. The calculation is based on the average solvation number, n_s, in Fig. 3(a) and the degree of ionic dissociation, α, in Fig. 8 in the main text.

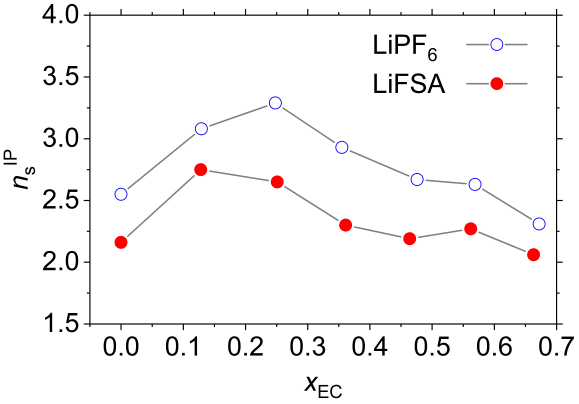

Figure S 2: Number of solvent molecules (EC+DMC) solvating one ion pair [$Li^+ \cdot A^-$] (A^- = PF_6^- or FSA^-) by assuming that Li^+ free from A^- is solvated by four solvent molecules. The fraction of ion pair in the system was calculated as $(1-\alpha)$ where α is the degree of dissociation given in Fig. 8.

Fig. S 3 plots the free energy change, ΔG, of the equilibrium

$$\mathrm{EC} \cdot \mathrm{Li}^+ + \mathrm{DMC} \overset{K}{\rightleftharpoons} \mathrm{DMC} \cdot \mathrm{Li}^+ + \mathrm{EC} \tag{S3}$$

where $\mathrm{EC} \cdot \mathrm{Li}^+$ and $\mathrm{DMC} \cdot \mathrm{Li}^+$ represent EC and DMC solvating Li^+, respectively, of which the number is N_s, and EC and DMC for the solvent molecules free from Li^+, of which the number is N_f, is given by

$$\Delta G = -RT \ln K = -RT \ln \frac{N_{\mathrm{s,DMC}} N_{\mathrm{f,EC}}}{N_{\mathrm{s,EC}} N_{\mathrm{f,DMC}}}. \tag{S4}$$

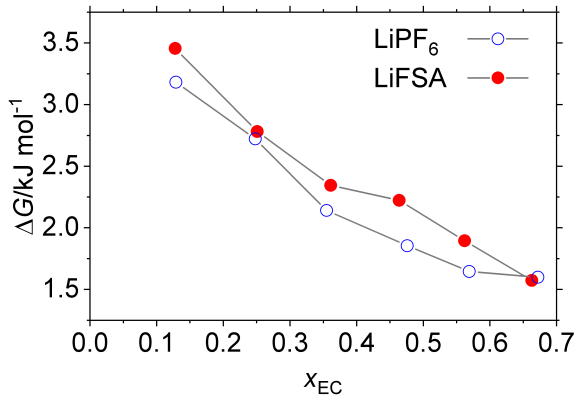

Figure S 3: Apparent free energy change, ΔG, associated with the equilibrium (S3).

The EC-preference over DMC $P^{\mathrm{B}}_{\mathrm{EC/DMC}}$ calculated from the data given by Bogle *et al.*[6] is shown in Fig. S 4. The data used are the number of carbonates molecules, N_{EC} and N_{DMC}, "associated with Li^+" given in Table 1 of their article based on Eq. (S5)..

$$P^{\mathrm{B}}_{\mathrm{EC/DMC}} \equiv \frac{N_{\mathrm{EC}}}{N_{\mathrm{DMC}}} \cdot \frac{1 - x_{\mathrm{EC}}}{x_{\mathrm{EC}}}. \tag{S5}$$

The numbers, N_{EC} and N_{DMC}, determined in their study involve the solvent in the secondary solvation shell. This result suggests that DMC is more populated than EC in a greater solvation environment around Li^+.

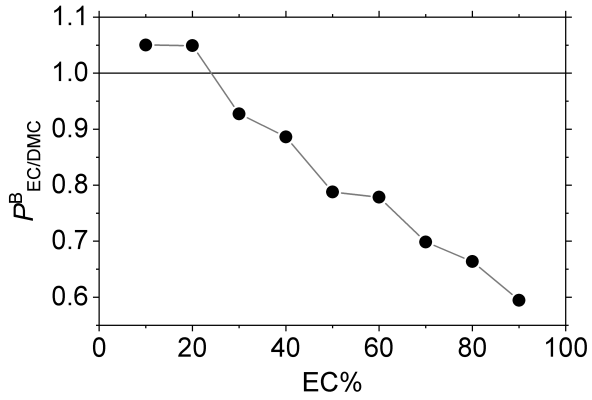

Figure S 4: EC-preference calculated from the data given in the ^{17}O NMR study by Bolgle *et al.*[6] for the 1 mol dm^{-3} $LiPF_6$ in the EC/DMC system.

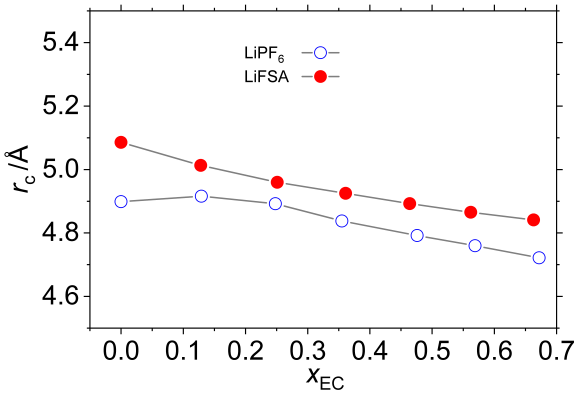

Figure S 5: Average radius of the Li^+ coordinated by the solvent and anion, r_{c}, calculated from the average solvation number, n_{s}, and the molar volume of the solvents and anions, V_{m}, using Eq. (16).

S 3 Apparent activation energy

Fig. S 6 plots the apparent activation energy, E_a, associated with the viscosity and conductivity calculated from their temperature dependency over $288 \leq T/\mathrm{K} \leq 338$ based on the Arrhenius relations

$$-\ln \eta = -\frac{E_a^\eta}{RT} + C_\eta \tag{S6}$$

$$\ln \sigma = -\frac{E_a^\sigma}{RT} + C_\sigma, \tag{S7}$$

where C_η and C_σ are constant.

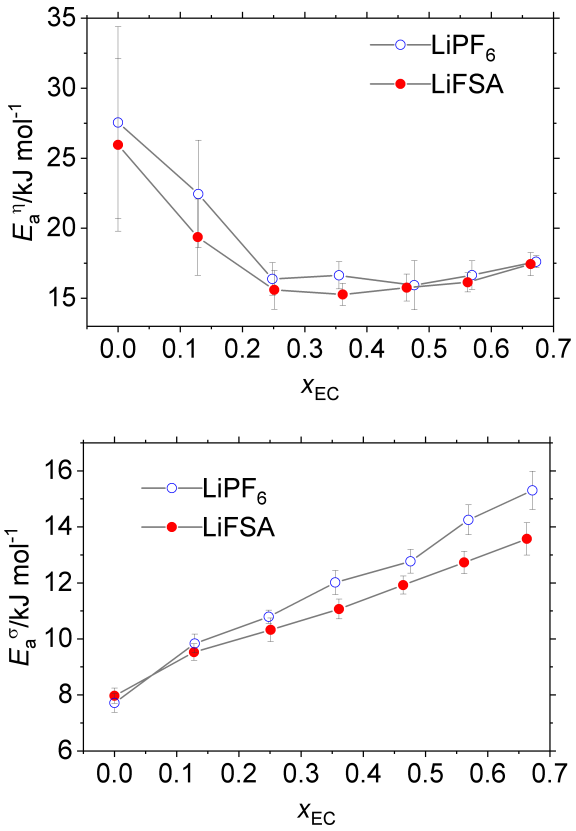

Figure S 6: Activation energy (a) E_a^η and (b) E_a^σ associated with viscosity and conductivity, respectively, from the temperature dependencies listed in Tables S II and S III, respectively. The error bars indicate twice the standard error $\pm 2\sigma$ in the slope determined by the linear optimization based on Eqs. (S6) and (S7).

S 4 PGSE NMR

As described in the Experimental sections, diffusion coefficient, D, was determined from the slope of the logarithmic relative spin-echo intensity $\ln(M/M_0)$ by varying pulse width of the field gradient, δ. Probed nuclides are ^{7}Li for Li^+, ^{19}F for PF_6^- and FSA^-, and ^{1}H for EC and DMC. An example is shown in Fig. S 7. The slopes of the lines give $-D$.

$$\ln\left(\frac{M}{M_0}\right) = -\left(\frac{\gamma\delta g}{\pi}\right)^2 (4\Delta - \delta)\, D \tag{S8}$$

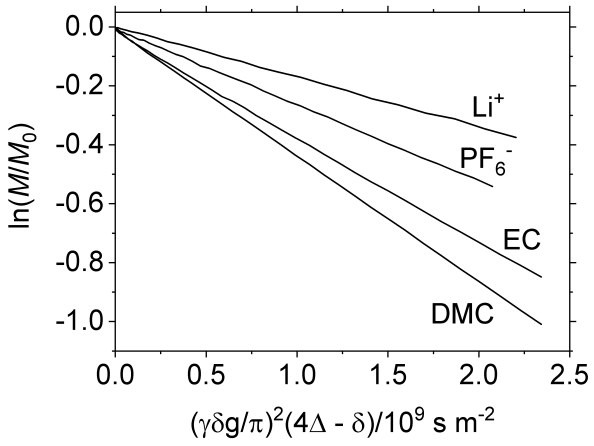

Figure S 7: Example of the relative spin-echo intensity, $\ln(M/M_0)$, as a function of $(\gamma\delta g/\pi)^2(4\Delta - \delta)$: $LiPF_6$ at $x_{EC} = 0.55$.

S 5 Stokes radius

$$r_{St,\alpha} = \frac{kT}{c\pi\eta D_\alpha} \tag{S9}$$

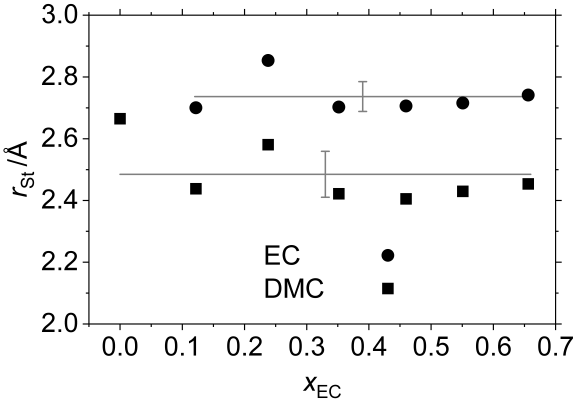

Figure S 8: Stokes radius of EC and DMC in solvent without solute calculated from the diffusion coefficient of each molecule and the solvent viscosity, η, based on Eq. (S9) where the shape factor is $c = 3.5$. The horizontal lines and vertical bars indicate the mean and twice the standard error, respectively.